Radiotherapy and Oncology 138 (2019) 166–172

Contents lists available at ScienceDirect

Radiotherapy and Oncology

journal homepage: www.thegreenjournal.com

Original Article

Deep learning derived tumor infiltration maps for personalized target definition in Glioblastoma radiotherapy

Jan C. Peeken [a,b,c,*], Miguel Molina-Romero [d], Christian Diehl [a], Bjoern H. Menze [d], Christoph Straube [a,b], Bernhard Meyer [e], Claus Zimmer [f], Benedikt Wiestler [f,1], Stephanie E. Combs [a,b,c,1]

[a] Department of Radiation Oncology, Klinikum rechts der Isar, Technical University of Munich (TUM); [b] Deutsches Konsortium für Translationale Krebsforschung (DKTK), Partner Site Munich; [c] Institute of Radiation Medicine (IRM), Department of Radiation Sciences (DRS), Helmholtz Zentrum München, Neuherberg; [d] Department of Computer Science, Image-Based Biomedical Modeling, Technical University of Munich (TUM), Garching; [e] Department of Neurosurgery; and [f] Department of Diagnostic and Interventional Neuroradiology, Klinikum rechts der Isar, Technical University of Munich (TUM), Germany

ARTICLE INFO

Article history:
Received 14 December 2018
Received in revised form 18 June 2019
Accepted 20 June 2019
Available online 11 July 2019

Keywords:
Glioblastoma
Deep learning
Radiotherapy
Personalized medicine
Diffusion tensor imaging
Tissue volume maps

ABSTRACT

Purpose: Glioblastoma is routinely treated by concomitant radiochemotherapy. Current target definition guidelines use anatomic MRI (magnetic resonance imaging) scans, taking into account contrast enhancement and the rather unspecific hyperintensity on the fluid-attenuated inversion recovery (FLAIR) sequence.

Methods and materials: We applied deep learning based free water correction of diffusion tensor imaging (DTI) scans to estimate the infiltrative gross tumor volume (iGTV) inside of the FLAIR hyperintense region. We analyzed the resulting iGTVs and their impact on target volume definition in a retrospective cohort of 33 GBM patients.

Results: iGTVs were significantly smaller compared to standard pre- and post-operative gross tumor volume (GTV) definitions. Two novel infiltrative tumor GTVs ($nGTV_{PRE\text{-}OP}$ and $nGTV_{POST\text{-}OP}$) defined as the conjunction volume of the standard GTV and the iGTV showed only a moderate increase in size compared to standard GTV definitions. On postoperative scans, the iGTV was predominantly covered by the two clinical target volume (CTV) concepts CTV_{EORTC} and CTV_{ROTG1}. A novel infiltrative tumor CTV (nCTV) [$nGTV_{POST\text{-}OP}$ + 2 cm margin] was significantly smaller compared to CTV_{ROTG1} but larger than CTV_{EORTC}. The overlap volume and conformity index demonstrated a distinct spatial configuration of the nCTV. Tumor recurrences overlapped with the iGTV in all but one patients and were completely covered by the nCTV in all patients. After reducing the margin to 1 cm recurrences coverage was at least in-field in all patients.

Conclusion: To conclude, free water corrected DTI scans may help to define infiltrative tumor areas of GBM that could ultimately be used to individualize RT treatment planning in terms of dose sparing or dose escalation.

Glioblastoma (GBM) is the most frequent malignant primary brain tumor. Current therapy regiments include gross tumor resection of the contrast enhancing tumor followed by radiotherapy (RT) with concomitant and adjuvant temozolomide [1]. The success of therapy, however, remains limited with a reported 5-year survival rate of 10.8% [2].

In RT planning, no definite contouring guideline has been established so far, and two major guidelines exist in parallel. The consensus guidelines of the European Organization for Research and Treatment of Cancer (EORTC) recommend targeting a clinical target volume (CTV) including the surgical resection cavity and any residual enhancing tumor defined on post-contrast T1

Abbreviations: CTV, clinical target volume; CE, contrast enhancement; DTI, diffusion tensor imaging; EORTC, European Organization for Research and Treatment of Cancer; ESTRO, European Society for Radiotherapy and Oncology; FA, fractional anisotropy; GBM, glioblastoma; GTV, gross tumor volume; iGTV, infiltrative gross tumor volume; MRI, magnetic resonance imaging; nGTV, novel gross tumor volume; nCTV, novel clinical target volume; PET, positron emission tomography; PTV, planning target volume; RT, radiotherapy; RTOG, Radiotherapy and Oncology Group; TV, tissue volume.

* Corresponding author at: Klinik für RadioOnkologie und Strahlentherapie, Universitätsklinikum rechts der Isar, Technische Universität München (TUM), Ismaninger Straße 22, 81675 München, Germany.

E-mail address: jan.peeken@tum.de (J.C. Peeken).

[1] BW and SEC contributed equally.

https://doi.org/10.1016/j.radonc.2019.06.031
0167-8140/

weighted MRI scans plus a 2 cm margin (CTV_{EORTC}) up to a total RT dose of 60 Gy in 30 fractions [1,3].

In contrast, the Radiotherapy and Oncology Group (RTOG) recommends a 2-phase approach adding surrounding edema defined on T2-weighted or Fluid Attenuated Inversion Recovery (FLAIR) scans to the resection cavity and any residual enhancing tumor plus a 2 cm margin (CTV_{RTOG1}) with the delivery of 46 Gy total RT dose in 23 fractions. Subsequently, an RT boost is given to a CTV_{EORTC} equivalent target volume up to a total RT dose of 60 Gy in 30 fractions [3,4]. Besides this, the European Society for Radiotherapy and Oncology (ESTRO) Advisory Committee on Radiation Oncology Practice (ESTRO-ACROP) established a third possibility, which defines the CTV according to the CTV_{EORTC}, but allows an adaption to include the adjacent FLAIR hyperintensities in selected cases. Noteworthy, the FLAIR hyperintensities are not included into the GTV but are rather considered as an area of infiltration [3].

The rationale for current strategies was largely defined by postmortem histological findings and tumor recurrence analyses in a trade-off with neurotoxicity. For instance, tumor recurrences tend to occur around the resection cavity [5,6]. Within a distance of 2 cm or 3 cm around the resection cavity approximately 80% or 95% of recurrences were located, respectively [7–9]. Tumor infiltration appeared to happen along white matter tracks [8]. In histological analysis, tumor cells were found over large proportions of the brain in varying cell densities indicating glioma as an infiltrative disease [10].

Classically, GBM CTVs were originally defined by CT imaging or, more recently, by MRI using T1-weight and FLAIR sequences. Recent advances in functional MRI, however, may allow even for more precise definitions of infiltrative tumor volume.

Diffusion tensor imaging (DTI) has emerged as a promising sequence for visualizing tumor infiltration and recurrence [11]: In a recent study from our institution, GBM recurrence preferably occurred in areas of reduced fractional anisotropy (FA), a measure derived from DTI data. Analysis of DTI is however complicated by edema, as the free water signal is superimposed over the diffusion signal. In order to separate these two signal sources, several algorithms have been proposed [12,13]. We have recently proposed a novel, deep learning based method for free water elimination of DTI [14]: Compared to existing implementations, our method allows for a fast, voxel-wise deconvolution of the raw tissue DTI signal, and additionally outputs tissue volume maps, which voxel-wise depict the ratio of tissue and free water diffusion. Preliminary analyses suggest that these maps may delineate tumor infiltration [14].

In this study, we defined infiltrative tumor volumes (iGTV) using tissue volume (TV) maps and free water corrected FA maps. The coverage in current contouring strategies was analyzed. We generated a novel gross tumor volume (nGTV) incorporating the iGTV. Finally, a novel CTV concept was defined. The respective planning volumes were correlated to tumor recurrences.

Materials and methods

We retrospectively analyzed all available 33 patients diagnosed with GBM that were treated with RT in our institution and that received pre-operative or postoperative DTI and anatomic (T1 ± contrast, T2, FLAIR) MRI scans (see Supplemental Material for MRI acquisition parameters). Pre-operative DTI scans were available in 24 patients, and postoperative DTI-scans were available in 21 patients. Both scans were available in 12 patients. The number of postoperative MRIs was limited as DTI hasn't been part of the standard postoperative protocol in our institution. Patient records were analyzed for RT regiments, demographics, tumor location, tumor recurrence, and MGMT promotor methylation status. This study was approved by the ethics committee of the Technical University of Munich (reference number 466/16).

The raw DTI data were exported as a 4D NIfTI and input into a neural network for signal deconvolution as described previously [14]. Briefly, the neural network was trained on simulated data to untangle "true" diffusion signal from free water corruption. This network outputs both the free water corrected DTI data, from which FA maps were calculated through the RESTORE algorithm [15], as well as tissue volume maps, which show the relative contribution of tissue and free water to the DTI signal in each voxel.

Treatment planning was performed in Aria Eclipse 13.0 (Varian, Mountain View, USA). All patients were treated following the guidelines of the ESTRO-ACROP consensus guidelines [3]. As consequence, the FLAIR hyperintensity region was included into the CTV if it was not already covered after the CTV expansion. CTV_{EORTC} was generated by adding a 2 cm margin to the resection cavity and residual contrast enhancing tumor based on postoperative T1-weighted contrast enhanced MRI scans. CTV_{RTOG1} was generated by adding a 2 cm margin to the resection cavity and residual contrast enhancing tumor as well as the FLAIR hyperintense region defined on postoperative MRI scans. Both CTVs were manually adapted to anatomic structures as described by the ESTRO-ACROP consensus guidelines [3].

Subsequent segmentation and analysis were performed using Slicer 3D (Version 4.8.0 stable release) [16]. To create tumor infiltration maps, the free water corrected FA maps were segmented using a threshold between the anisotropy levels of 0.2 and 0.35 and free water corrected TV maps were thresholded between 0.4 and 0.7 based on previous findings [14]. The Boolean overlap between both resulting maps and the FLAIR hyperintense regions was generated representing the iGTV. We defined a novel preoperative GTV ($nGTV_{pre\text{-}OP}$) as the conjunction volume of the iGTV and contrast enhancing GTV (GTV_{CE}). In the postoperative situation, the novel GTV ($nGTV_{POST\text{-}OP}$) was generated as the conjunction volume of the iGTV and the resection cavity and residual enhancing tumor (GTV_{cavity}). Two novel CTVs were defined by adding a 2 cm (nCTV) or 1 cm ($nCTV_{1cm}$) margin to the $nGTV_{POST\text{-}OP}$ as described above. nCTV1cm was analyzed as potential boost volume with a stronger dependence of the iGTV while still taking into account microscopic spread around the detectable iGTV. The coverage of tumor recurrences was classified by the percentage overlap with the respective CTV concept as central (>95% coverage), infield (81–95% coverage), marginal (20–80% coverage), or distant (<20% coverage) as previously described [17].

Volume size and dice similarity coefficients (DSC) were calculated using the DiceComputation module of the SlicerRT extension. The conformity index of two volumes of interest was calculated by dividing the intersection volume by the conjunction volume giving a measure for the spatial overlap of both volumes [18]:

$$Conformity\ Index: \frac{CTV(EORTC) \cap nCTV}{CTV(EORTC) \cup nCTV}$$

The overlap volume of two volumes was calculated by diving the intersection volume (e.g., CTV_{EORTC} and nCTV) by the volume of interest (e.g., nCTV) indicating its coverage by the other volume of interest (e.g., CTV_{EORTC}).

$$Overlap\ Volume: \frac{CTV(EORTC) \cap nCTV}{nCTV}$$

See Fig. 1 for an illustration of both volumetric measures. All statistical analyses were performed using GraphPad Prism version 5.0c (GraphPad Software Inc., La Jolla, CA, USA). The KS normality test was used to estimate if data were normally distributed. Students' *t*-test was used to compare planning volumes without correction for multiple testing. In cases of non-normally distributed data, the Mann–Whitney *U* test was used. A two-tailed

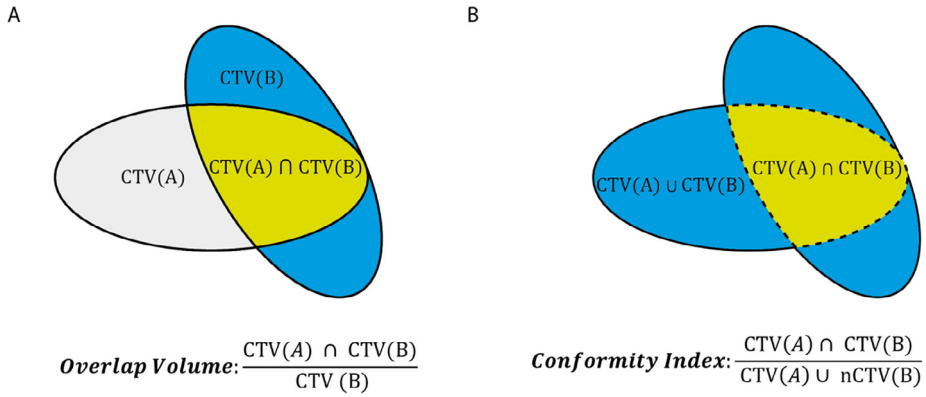

Fig. 1. Illustration of the overlap volume and conformity index. The overlap volume (A) is calculated by dividing the intersection volume of two volumes (yellow) by the volume of interest (CTV(B)) (blue). The conformity index (B) of two volumes of interest was calculated by dividing the intersection volume (yellow) by the conjunction volume (blue). (For interpretation of the references to color in this figure legend, the reader is referred to the web version of this article.)

p-value of less than 0.05 was regarded as statistically significant. A paired test was applied if measurements from the same patient cohort were compared.

Results

Patients

See Table 1 for patient demographics, tumor location, recurrence statistics, and MGMT promoter methylation status. In total, 28 (85%) patients were treated with up to a total dose radiation dose of 60 Gy in 2 Gy singles doses with concomitant temozolomide chemotherapy. Due to poor performance scores, five (15%) patients received hypofractionated RT up to a total dose of 40.05 Gy in 2.67 Gy single doses with concomitant temozolomide chemotherapy. All but one patient received tumor resection prior to RT.

Table 1
Patient characteristics.

Age		m 65 years (r: 29–85)	
KPS		70% (r: 30–100%)	
Gender	Male	24 p	72.7%
	Female	9 p	27.3%
MGMT-status	Methylated	7 p	21.2%
	Unmethylated	25 p	75.6%
	Unknown	1 p	3.0%
Tumor site	Left	19 p	57.5%
	Right	14 p	42.5%
Location	Frontal	11 p	33.3%
	Parietal	7 p	21.2%
	Temporal	9 p	27.2%
	Occipital	3 p	9.0%
	Thalamic	2 p	6.1%
	Frontotemporal	1 p	3.0%

label: m: median, KPS: Karnofsky Performance Score, MGMT: O-6-methylguanine DNA methyltransferase promoter, p: patients, r: range.

The infiltrative gross tumor volume (iGTV)

First, pre-operatively acquired DTI imaging was used to generate infiltrative tumor maps. The pre-operative iGTV had a median size of 7.8 cc (range 0.4–32.4 cc). This was significantly smaller compared to the GTV_{CE} (median size 23.3 cc, range 0.8–185.9 cc, $p = 0.0001$). The iGTV overlapped with the GTV_{CE} with a proportion of 50% (range 4–100%) reflecting that large proportions of the iGTV were located inside of the peritumoral FLAIR hyperintense region. Consequently, the $nGTV_{PRE\_OP}$ (median size 30.8 cc, range 1.9–187.2) had a median 32% greater volume compared to the GTV_{CE}.

In 22 patients with available postoperative imaging studies, DTI scans were used to generate postoperative iGTVs (see Fig. 2). In direct comparison in patients that had pre and post-operative DTI scans, tumor resection led to a smaller size of the post-operative iGTV, without reaching statistical significance (median 5.9 cc, range 1.3–29.0 cc, $p = 0.24$).

The iGTV was included inside of the GTV_{cavity} with a median proportion of 55% (range 4–100%). Compared to GTV_{cavity}, the $nGTV_{POST\_OP}$ showed a median 8% larger volume.

Pattern of recurrence

In total, 14 patients (42%) were diagnosed with tumor recurrence defined by the "response assessment in neuro-oncology" (RANO) criteria [19]. Six patients received tumor resection at recurrence. Histological work-up in these patients proved tumor recurrence in all of these cases. Recurrent tumor volumes intersected with the iGTVs in all patients but one (93% of all patients with recurrences). In this patient, the tumor recurrence occurred at the resection cavity inside of a FLAIR isointense region.

A novel CTV concept

Preoperative and postoperative iGTVs were predominantly covered by the CTV_{EORTC} with a median proportion of 97% (range 37–100%) and 100% (range 4–100%), respectively. As the iGTV was defined inside of the FLAIR hyperintense region, CTV_{RTOG1} covered all iGTVs completely.

Using the post-operative iGTVs we defined two novel infiltrative tumor CTVs. The nCTV was generated by adding a margin of 2 cm (nCTV) to $nGTV_{POST\text{-}OP}$ to account for microscopic spread (see Fig. 3 for exemplary cases with correlation to tumor recurrences). The resulting nCTVs had a median size of 240.9 cc (range 75.1–458.5 cc) and were significantly smaller compared to CTV_{RTOG1} (median 276.8 cc, range 142.0–480.2 cc) ($p = 0.045$) but larger than CTV_{EORTC} (median 207.2 cc, range 88.36–452.9 cc) ($p = 0.006$) (see Fig. 4).

Next, the spatial configuration of the nCTV was compared to the conventional CTV definitions (see Table 2). The nCTV overlapped with CTV_{EORTC} and CTV_{RTOG1} with a median intersection volume of 80% and 98%. The coverage was significantly different from a full overlap for CTV_{EORTC} ($p < 0.0001$) and CTV_{RTOG1} ($p < 0.0001$). The conformity index was significantly different from one for CTV_{EORTC} and CTV_{RTOG1} ($p < 0.0001$, each) indicating a distinct spatial

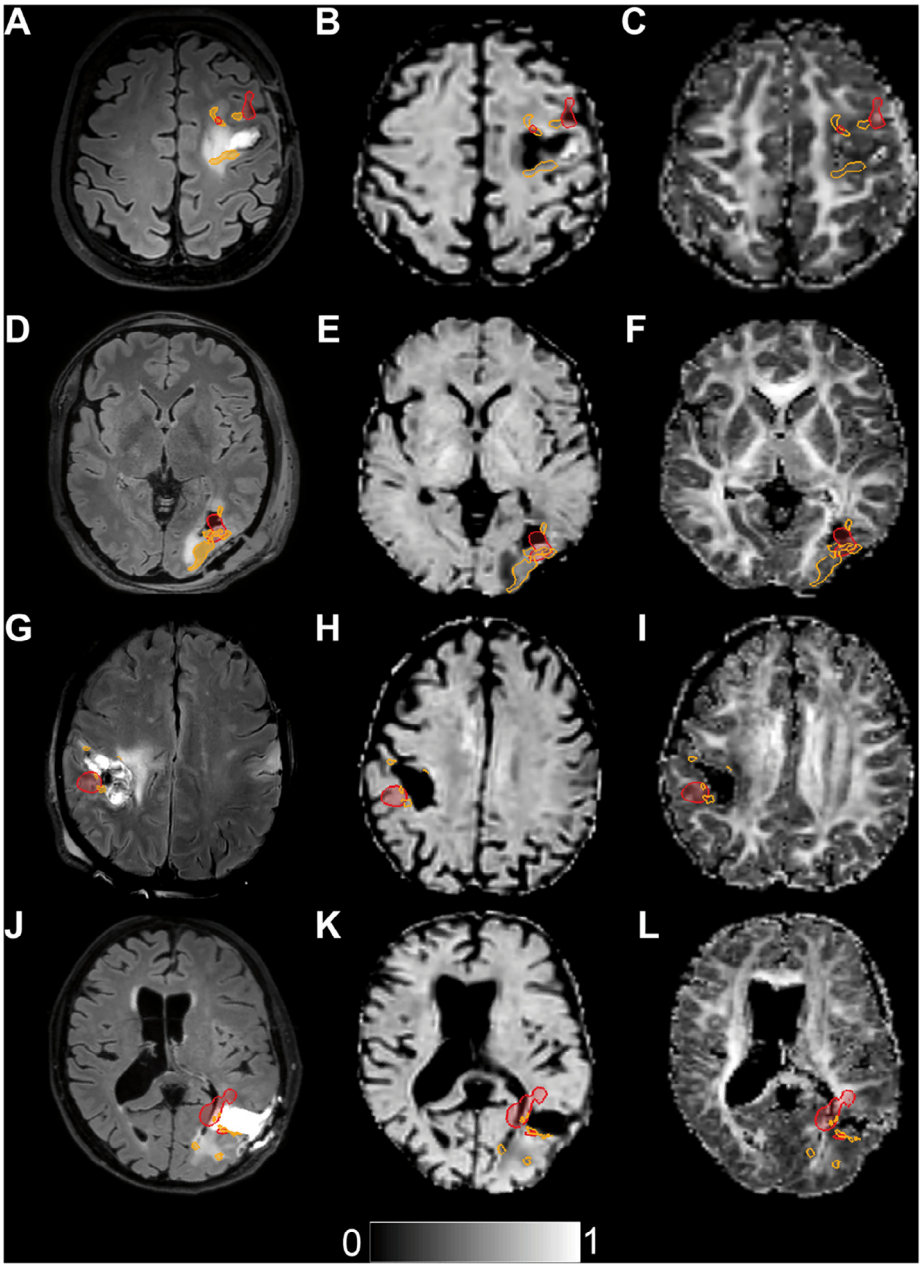

Fig. 2. Pattern of recurrence in comparison to the infiltrative gross tumor volume (iGTV) derived from free water corrected fractional anisotropy and tissue volume maps. Exemplary comparison of the tumor recurrence (red segmentation) registered to the post-operative fluid attenuated inversion recovery (FLAIR) MRI scans (A, D, G, J). The infiltrative gross tumor volume (iGTV) is depicted in orange. The respective free water corrected tissue volume (B, E, H, K), fractional anisotropy maps (C, F, I, L), and a representative greyscale are shown. (For interpretation of the references to color in this figure legend, the reader is referred to the web version of this article.)

distribution and geometrical shape. The median Dice similarity coefficients (DSC) of nCTV with CTV_{EORTC} and CTV_{RTOG1} were 0.88 and 0.95, respectively.

Coverage of recurrent GBM using the novel CTV concept

In all patients with postoperative CTVs all six tumor recurrences were covered by $CTV_{RTOG1,}$ CTV_{EORTC} and nCTV completely (central coverage). In addition, we created a potential boost volume ($nCTV_{1cm}$) by adding a 1 cm margin to the $nGTV_{POST-OP.}$ The $nCTV_{1cm}$ covered one recurrences in-field and the remaining cases centrally. For comparison, a 1 cm margin was added to the GTV_{cavity} in analogy to CTV_{EORTC} that covered three recurrences centrally ($CTV_{EORTC1cm}$). In two patients and one patient the recurrent GBMs were covered in-field or marginal, respectively.

Discussion

In this work, we introduced a novel concept of defining iGTVs using free water corrected TV and FA maps derived from DTI scans using deep learning. These newly defined subvolumes within the FLAIR hyperintense region may represent infiltrative tumor. We demonstrated that iGTVs were not completely covered inside of the current contrast enhanced MRI based GTV definition. Conjunction volumes including the standard GTVs plus the iGTV showed moderate increases in total volume, especially in the postoperative situation but also preoperatively. As the proposed method of GTV definition allows to define the residual infiltrating tumor volume more precisely than by simply including rough geometric estimates, we made a proposition for a novel CTV. The iGTV was added to the current standard GTV (resection cavity and the residual

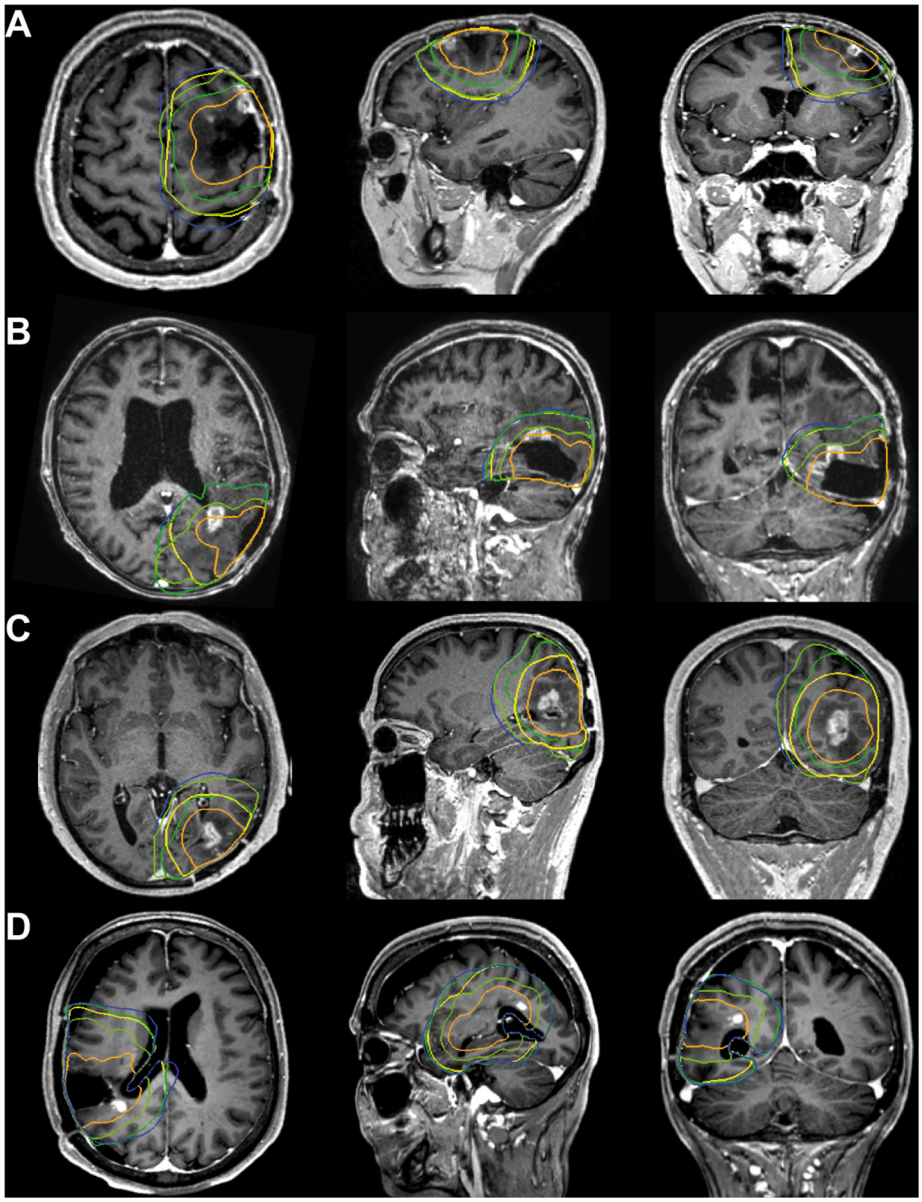

Fig. 3. Comparison of the nCTV with established CTV strategies. T1-weighted contrast-enhanced MRI scan depicting the respective tumor recurrence and the registration of the different CTV concepts. All four tumor recurrences (A–D) had histological confirmation and post-operative DTI scans available. The blue line depicts the CTV_{RTOG1}. The light green and dark green lines represent the nCTV and nCTV1cm (one centimeter safety margin). CTV_{EORTC} and $CTV_{EORTC1cm}$ (one centimeter safety margin) are represented by the yellow and orange lines. (For interpretation of the references to color in this figure legend, the reader is referred to the web version of this article.)

contrast enhancing tumor). The resulting nCTV had significantly larger volume compared to CTV_{EORTC} but smaller volume compared to CTV_{RTOG1} and was spatially different from them. Tumor recurrences overlapped with the iGTV and was covered by nCTV in all patients.

As described above, no optimal target delineation concept has been established worldwide. So far, no direct comparison between CTV definitions of the EORTC and RTOG guidelines were made in any prospective randomized trial. In two prospective international studies that allowed application of both concept, however, no significant difference in outcome was seen following randomization according to radiotherapy technique [4,20]. In other words, the inclusion and expansion of the whole FLAIR hyperintense region, which may include infiltrative tumor but also peritumoral edema, did not confer a prognostic benefit. The iGTV and nCTV concepts presented here aims for more precise, individualized tumor targeting inside of the FLAIR hyperintense region. It may be applied to multiple RT planning scenarios. For instance, the nCTV may supplement the FLAIR-positive region in a two CTV-concept. The reduction of the treatment volume may help to reduce neurotoxicity.

DTI data have shown promise for predicting tumor recurrence [11]. Estimating the voxel-wise tissue volume fraction from DTI data is a novel approach for visualizing tumor infiltration in the peritumoral region. In a previous analysis, we have found that the tissue volume fraction is substantially higher in areas of contrast enhancement as well as in peritumoral areas with suspicious T2 signal [14]. While this suggests that tissue volume may be a non-invasive measure of tumor infiltration, this has not been independently validated. To this end, we are currently investigating a cohort of GBM patients to systematically investigate the relation between tissue volume, free water corrected FA and tumor recurrence.

Several other approaches have been proposed to optimize GBM treatment planning. Amino acid-based positron emission tomogra-

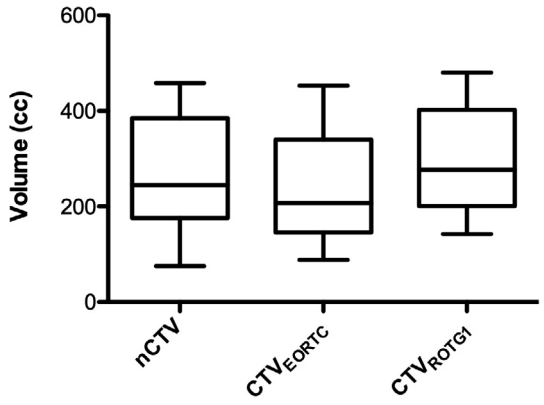

Fig. 4. A CTV size comparison. Comparison of CTV volumes of nCTV, CTV$_{EORTC}$, and CTV$_{RTOG1}$. nCTV was significantly smaller compared to CTV$_{RTOG1}$ but larger than CTV$_{EORTC}$ ($p = 0.045$ and $p = 0.006$, respectively, by two-sided paired Students' *t*-test).

Table 2
Comparison of the novel CTV (nCTV) with clinical target volumes.

	CTV$_{EORTC}$	CTV$_{RTOG1}$
Overlap volume	0.80 (0.5–1.0)	0.98 (0.51–1.0)
Conformity index	0.76 (0.46–0.98)	0.92 (0.43–0.96)
Dice similarity coefficient	0.88 (0.66–0.99)	0.95 (0.61–0.99)

Overview of the overlap volume, conformity index and dice similarity coefficient (also see Fig. 2 for a schematic overview) of the nCTV with CTV$_{EORTC}$ and CTV$_{RTOG1}$. The median values are shown. The range is listed in parentheses.

phy (PET) uptake can be used to assess the cancerous metabolism enabling prognostic assessment, non-invasive tumor grading but also improved postoperative gross tumor assessment [21,22]. RT planning studies showed major differences in GTV definition compared to the standard MRI-based technique [18,23,24]. Whole Brain Spectroscopy which was correlated to GBM tumor cell density may constitute an alternative way to assess tumor infiltration [25]. Finally, the mathematical modeling of tumor growth on the basis of estimated tumor cell density was used to adjust CTVs [26]. Combining these approaches directly or using it as input for an optimal mathematical growth modeling may help to find the best approach. In a first step, we recently demonstrated a tumor growth model using (18)F-fluoro-ethyl-tyrosine PET biological tumor volumes as input feature [27].

Early dose escalation studies have shown controversial results showing a high proportion of in-field recurrences despite total RT doses of 90 Gy delivered by 3D conformal RT [28]. In a recent study, however, dose escalation up to 81 Gy total RT dose to the resection cavity plus enhancing residual tumor using intensity modulated RT with concomitant temozolomide showed a promising median overall survival of 20.1 months [29]. Recurrence analysis showed that insufficient coverage of pre-therapeutic 11C-methionine PET-based tumor volumes was associated with a higher risk of non-central failure [29]. These controversial results might be explainable by an insufficient target volume definition, which focused on contrast enhancement. Besides PET imaging, the iGTV introduced here could represent an additional technique for defining areas of infiltration that should be included into the high-dose target volume in dose escalation trials. For example, the reduced margin CTV$_{1cm}$ could be used as target volume for dose escalation. In our study, nCTV$_{1cm}$ covered all postoperative recurrences at least in-field. In contrast, a CTV in analogy to CTV$_{EORTC}$ using a 1 cm margin showed a marginal coverage in one patient. As can be expected from the frequent recurrences close to the resection cavity, all recurrences were completely covered by CTV$_{EORTC}$ [7–9]. As consequence, validation of iGTVs and distant recurrences is indicated. To this end, future studies should assess the true value of iGTV based recurrence prediction and its value for treatment planning with a larger patient cohort.

The presented data bear several limitations. To enable a first analysis, preoperative DTI scans were used to test the concept of iGTVs, bringing about limitations: First, surgery leads to a significant anatomical shift, making a correct registration to postoperative planning MRI or CT scans difficult. Secondly, interim tumor growth between pre-operative imaging and RT planning could not be accounted for. To address these issues, we sought patients with postoperative DTI scans. As GBM patients did not regularly receive post-operative DTI imaging in our institution, the resulting patient number was limited. In addition, postoperative hemorrhage and present ischemia challenges for DTI. Thirdly, FA values in normal brain tissue show a heterogeneous distribution [30]. As consequence, the proposed method remains restricted to the FLAIR hyperintense regions and thus may miss tumor infiltration in FLAIR-isointense brain tissue as could be observed in one patient in this study. Further on, regional variations of FA and TV intensities may lead to unspecific iGTV segmentations. Manual adaption of the resulting volumes regarding known infiltration routes, e.g. along fiber tracts, may help to increase the precision of the method in future studies. Lastly, the calculated maps may suffer from some distortion which should be accounted for by an appropriate safety margin. As a consequence, the available number of tumor recurrences was limited, too. Future studies should prospectively address these issues using postoperative MRIs only.

To conclude, with the help of deep learning-based free water correction of DTI imaging, we generated a novel concept for an iGTV. We generated a novel nCTV with significantly different size and shape parameters compared to CTV$_{EORTC}$ and CTV$_{ROTG1}$. The novel nCTV and nCTV$_{1cm}$ showed good coverage of tumor recurrences. The proposed concepts may be used as the basis for more precise GBM RT targeting.

Funding

This research was funded by Deutsches Konsortium für Translationale Krebsforschung (DKTK), Medical Faculty of the Technical University of Munich (KKF Physician Scientist Program), Deutsche Forschungsgemeinschaft (DFG) (SFB 824) and Helmholtz Zentrum Munich.

Acknowledgment

None.

Declaration of Competing Interest

The authors declare no conflict of interest.

Disclosure

All authors concur with the submission and none of the data have been published or are under consideration elsewhere.

Appendix A. Supplementary data

Supplementary data to this article can be found online at https://doi.org/10.1016/j.radonc.2019.06.031.

References

[1] Stupp R, Mason WP, van den Bent MJ, et al. Radiotherapy plus concomitant and adjuvant temozolomide for glioblastoma. N Engl J Med 2005;352:987–96. https://doi.org/10.1056/NEJMoa043330.

[2] Stupp R, Hegi ME, Mason WP, et al. Effects of radiotherapy with concomitant and adjuvant temozolomide versus radiotherapy alone on survival in glioblastoma in a randomised phase III study: 5-year analysis of the EORTC-NCIC trial. Lancet Oncol 2009;10:459–66. https://doi.org/10.1016/S1470-2045(09)70025-7.
[3] Niyazi M, Brada M, Chalmers AJ, et al. ESTRO-ACROP guideline "target delineation of glioblastomas". Radiother Oncol 2016;118:35–42. https://doi.org/10.1016/j.radonc.2015.12.003.
[4] Gilbert MR, Wang M, Aldape KD, et al. Dose-dense temozolomide for newly diagnosed glioblastoma: a randomized phase III clinical trial. J Clin Oncol 2013;31:4085–91. https://doi.org/10.1200/JCO.2013.49.6968.
[5] Bashir R, Hochberg F, Oot R. Regrowth patterns of glioblastoma multiforme related to planning of interstitial brachytherapy radiation fields. Neurosurgery 1988;23:27–30. https://doi.org/10.1227/00006123-198807000-00006.
[6] Bette S, Barz M, Huber T, et al. Retrospective analysis of radiological recurrence patterns in glioblastoma, their prognostic value and association to postoperative infarct volume. Sci Rep 2018;8:1–12. https://doi.org/10.1038/s41598-018-22697-9.
[7] Wallner KE, Galicich JH, Krol G, Arbit E, Malkin MG. Patterns of failure following treatment for glioblastoma multiforme and anaplastic astrocytoma. Int J Radiat Oncol 1989;16:1405–9. https://doi.org/10.1016/0360-3016(89)90941-3.
[8] Halperin EC, Bentel G, Heinz ER, Burger PC. Radiation therapy treatment planning in supratentorial glioblastoma multiforme: an analysis based on post mortem topographic anatomy with ct correlations. Int J Radiat Oncol 1989;17:1347–50. https://doi.org/10.1016/0360-3016(89)90548-8.
[9] Aydın H, Sillenberg I, von Lieven H. Patterns of failure following CT-based 3-D irradiation for malignant glioma. Strahlenther Onkol 2001;177:424–31. https://doi.org/10.1007/PL00002424.
[10] Capper D. Addressing diffuse glioma as a systemic brain disease with single-cell analysis. Arch Neurol 2012;69:523. https://doi.org/10.1001/archneurol.2011.2910.
[11] Bette S, Huber T, Gempt J, et al. Local fractional anisotropy is reduced in areas with tumor recurrence in glioblastoma. Radiology 2017;283:499–507. https://doi.org/10.1148/radiol.2016152832.
[12] Hoy AR, Koay CG, Kecskemeti SR, Alexander AL. Optimization of a free water elimination two-compartment model for diffusion tensor imaging. Neuroimage 2014;103:323–33. https://doi.org/10.1016/j.neuroimage.2014.09.053.
[13] Pasternak O, Sochen N, Gur Y, Intrator N, Assaf Y. Free water elimination and mapping from diffusion MRI. Magn Reson Med 2009;62:717–30. https://doi.org/10.1002/mrm.22055.
[14] Molina-Romero M, Wiestler B, Gomez P, Menzel M, Menze B. Deep learning with synthetic diffusion MRI data for free-water elimination in glioblastoma cases. Miccai 2018.
[15] Chang L-C, Jones DK, Pierpaoli C. RESTORE: Robust estimation of tensors by outlier rejection. Magn Reson Med 2005;53:1088–95. https://doi.org/10.1002/mrm.20426.
[16] Fedorov A, Beichel R, Kalphaty-Cramer J, et al. 3D slicers as an image computing platform for the quantitative imaging network. Magn Reson Imaging 2012;30:1323–41. https://doi.org/10.1016/j.mri.2012.05.001.3D.
[17] McDonald MW, Shu HKG, Curran WJ, Crocker IR. Pattern of failure after limited margin radiotherapy and temozolomide for glioblastoma. Int J Radiat Oncol Biol Phys 2011;79:130–6. https://doi.org/10.1016/j.ijrobp.2009.10.048.
[18] Niyazi M, Geisler J, Siefert A, et al. FET-PET for malignant glioma treatment planning. Radiother Oncol 2011;99:44–8. https://doi.org/10.1016/j.radonc.2011.03.001.
[19] Wen PY, Macdonald DR, Reardon DA, et al. Updated response assessment criteria for high-grade gliomas: Response assessment in neuro-oncology working group. J Clin Oncol 2010;28:1963–72. https://doi.org/10.1200/JCO.2009.26.3541.
[20] Stupp R, Hegi ME, Gorlia T, et al. Cilengitide combined with standard treatment for patients with newly diagnosed glioblastoma with methylated MGMT promoter (CENTRIC EORTC 26071–22072 study): a multicentre, randomised, open-label, phase 3 trial. Lancet Oncol 2014;15:1100–8. https://doi.org/10.1016/S1470-2045(14)70379-1.
[21] Pyka T, Gempt J, Hiob D, et al. Textural analysis of pre-therapeutic [18F]-FET-PET and its correlation with tumor grade and patient survival in high-grade gliomas. Eur J Nucl Med Mol Imaging 2016;43:133–41. https://doi.org/10.1007/s00259-015-3140-4.
[22] Poulsen SH, Urup T, Grunnet K, et al. The prognostic value of FET PET at radiotherapy planning in newly diagnosed glioblastoma. Eur J Nucl Med Mol Imaging 2016:1–9. https://doi.org/10.1007/s00259-016-3494-2.
[23] Grosu AL, Weber WA, Astner ST, et al. 11C-methionine PET improves the target volume delineation of meningiomas treated with stereotactic fractionated radiotherapy. Int J Radiat Oncol Biol Phys 2006;66:339–44. https://doi.org/10.1016/j.ijrobp.2006.02.047.
[24] Harat M, Małkowski B, Makarewicz R. Pre-irradiation tumour volumes defined by MRI and dual time-point FET-PET for the prediction of glioblastoma multiforme recurrence: a prospective study. Radiother Oncol 2016;120:241–7. https://doi.org/10.1016/j.radonc.2016.06.004.
[25] Cordova JS, Shu HKG, Liang Z, et al. Whole-brain spectroscopic MRI biomarkers identify infiltrating margins in glioblastoma patients. Neuro Oncol 2016;18:1180–9. https://doi.org/10.1093/neuonc/now036.
[26] Unkelbach J, Menze BH, Konukoglu E, et al. Radiotherapy planning for glioblastoma based on a tumor growth model: improving target volume delineation. Phys Med Biol 2014;59:747. https://doi.org/10.1088/0031-9155/59/3/771.
[27] Lipkova J, Angelikopoulos P, Wu S, et al. Personalized radiotherapy design for glioblastoma: integrating mathematical tumor models, multimodal scans and bayesian inference. IEEE Trans Med Imaging 2019:1. https://doi.org/10.1109/TMI.2019.2902044.
[28] Chan JL, Lee SW, Fraass BA, et al. Survival and failure patterns of high-grade gliomas after three-dimensional conformal radiotherapy. J Clin Oncol 2002;20:1635–42. https://doi.org/10.1200/JCO.2002.20.6.1635.
[29] Tsien CI, Brown D, Normolle D, et al. Concurrent temozolomide and dose-escalated intensity-modulated radiation therapy in newly diagnosed glioblastoma. Clin Cancer Res 2012;18:273–9. https://doi.org/10.1158/1078-0432.CCR-11-2073.
[30] Brander A, Kataja A, Saastamoinen A, et al. Diffusion tensor imaging of the brain in a healthy adult population: Normative values and measurement reproducibility at 3 T and 1.5 T. Acta Radiol 2010;51:800–7. https://doi.org/10.3109/02841851.2010.495351.